

STATIONARY CAVITONS IN A MAGNETIC MIRROR

A.J. Balloni

Dr. J. Busnardo Neto

CTA/IEAV

UNICAMP / IF

We report the experimental observation of cavitons in an Argon plasma, produced and heated by an rf field and confined by a magnetic mirror system. The cavitons are simultaneously observed in the electron density N_e (dip), the electron temperature T_e (peak), the floating potential V_f (dip) and in the rf fields (peak). They are stable in time, sharply localized and stationary in space and there is equilibrium between the ponderomotive and the thermokinetic forces. Their widths is of the order 2.0 to 4.0 cm, $\Delta N_e/N_e \approx -100\%$ and $\Delta T_e/T_e \approx 200\%$.

magnetized Lisitano plasma where the electron temperature T_e is much higher than the ion temperature T_i (8,9). The plasma is produced and heated by a radio frequency (rf) field in continuous mode, differently from previous work, where an oscillating quasi-static electric field was applied to an unmagnetized plasma with a density gradient prepared before hand (4, 10). Our experimental apparatus permits reliable measurements in the presence of the rf field. The observed nonlinear structure (cavitons) are highly stable (in time) and localized (in space) at some position which depends on the plasma conditions as pressure or magnetic field strength.

2. EXPERIMENTAL SETUP

The magnetic mirror system is constructed from six coils located at equal distances around a glass cylinder of radius $r=8.5\text{cm}$ and length $L=160.0\text{cm}$ (cf. figure 1 in references (1, 11)). The strength of the magnetic field on the cylinder axis can be varied from 0.0 to 0.32 T and the magnetic field lines are shown in figure 2 (cf. references (1, 11)). The argon plasma is generated with the rf wave, with the mirror magnetic field off. The rf field has a frequency $\omega_{rf}=120\text{ MHz}$ and is produced by a ceramic tube amplifier, which operates with an output power up to 600W in continuous wave mode. The heart of the rf coupling device to the plasma is a rf helix with the following dimensions: diameter of the helix conductor $d=0.2\text{cm}$, diameter of the helix $D=8.82\text{cm}$, circumference $C=27.7\text{cm}$, space between turns $S=1.25\text{cm}$, turn length $L=27.74\text{cm}$, and pitch angle $\theta=2.58^\circ$ (12). It is wound in 11 turns outside around the central region of the cylinder and connected to a coaxial transmission line. With the mirror magnetic field off, the plasma appears only in the two central cells; with the magnetic field on, the plasma is confined in the central region of the glass tube, and appears in all cells, (figure 1 of

1 - INTRODUCTION

During the last years the study of low temperature plasmas physics in a magnetic mirror has produced interesting results such as the observation of ionization waves (1), and radio frequency heating (2,3). In this work we want to present another application of a magnetic mirror system, which lead us to the experimental observation of stationary cavitons.

The formation of cavitons has been observed since the early seventies (4) and explained theoretically (5). An oscillating pump electric field of frequency ω_{rf} , directed along a density gradient, drives an electrostatic resonance near the point where the plasma frequency $\omega_{pe}(z)$ is equal to the radio frequency ω_{rf} . The resonance gives rise to density cavities driven by a ponderomotive force. However, the cavities propagate down the gradient and away from the resonance and are transient on the ion time scale (6,7).

In the present work, we use a

reference (1,11)).

A diffusion vacuum pump at one end of the cylinder keeps the pressure constant during the discharge (approximately 1 to $4 \cdot 10^{-4}$ Torr against a background pressure of the 10^{-6} Torr).

The diagnostics used were: A planar Langmuir probe which could be moved along the axial (Z) direction, on the cylinder axis. The probe signal is fed to a dc circuit through a low-pass filter. The others diagnostic used were: a magnetic probe, a double tip-probe and a gaussmeter (W.M.S.). These diagnostic were extensively discussed in references (1,11). Multiple mirrors were used to eliminate edge effects on the plasma, produced by the stainless steel flanges at each end of the vessel (1).

3. EXPERIMENTAL RESULTS

We have studied the plasma at pressures $P = 1.0, 2.0, 3.0$ and 3.5×10^{-4} Torr and mean mirror magnetic fields $\bar{B} = (B_{\max} + B_{\min})/2 = 3.7, 5.5, 8.1, 14.2$ and 21.0×10^{-2} T. In each of the resulting 20 combinations of P and B we have measured the Langmuir probe voltage-current characteristic as well as the components E_z, B_z, E_r and E_ϕ of the rf electromagnetic field between the points F and G, i.e., in the interval $0.0 \leq Z \leq 26.0$ cm in steps of 1.0 cm and at radial positions $r = 0.0$ cm, cf. figure 2 of references (1,11). These measurements with the Langmuir probe have been repeated at least 6 (six) times at each centimeter, from point F to point G on the cylinder axis. Their Gaussian mean value was calculated and the error is less than 20%.

From the Langmuir probes characteristics we calculate the electron temperature T_e , the electron density N_e , the floating potential V_f and the plasma potential V_p in the standard way (13). Since the radio frequency W_{rf} is lower than the electron plasma frequency W_{pe} , the probe characteristics must be corrected (2). When a rf field E_{rf} , used to produce and heat the plasma, is applied on the Langmuir probe inside the plasma, the rf voltage V_{rf} on the probe, for example, decrease the floating potential $V_f(0)$ to $V_f(V_{rf})$. In the case of a Maxwellian distribution for the electrons this variation is given by $\Delta V_f = [V_f(0) - V_f(V_{rf})] = T_e \ln [I_0(eV_{rf}/KbT_e)]$, where I_0 is the zeroth-order modified Bessel function, and Kb is the Boltzmann constant. For the ranges of T_e and V_{rf} in this work the variation ΔV_f is less than 1% with respect to $V_f(0)$. Corrections of the same order occur for the quantities T_e, N_e and V_p , therefore we can say that the Langmuir probe diagnostic has not been affected by the rf field.

Our principal result is that at certain spatial positions $Z = Z^L(P, B)$ a sharp maximum of T_e, E_r, E_z, B_r, B_z and E_ϕ , and a sharp minimum of N_e and V_f are observed. The extremum values of $T_e (Z^L)$ and their positions Z^L as well as the average values of T_e and N_e are shown in table I.

As an example we show the results obtained for $P = 3.0 \times 10^{-4}$ Torr and $B = 3.7 \times 10^{-2}$ T. The quantities T_e and N_e are shown as function of Z in figure 1, E_r and E_z in figure 2. Since $|E_{rf}| \ll |B_{rf}|$ the energy density U_{rf} is approximately given by $U_{rf} \approx |B_{rf}|^2/8\pi$ and shows a qualitatively similar behavior as figure 2.

The results for $P = 3.5, 3.0, 2.0$ and 1.0×10^{-4} Torr indicate that the formation of the extremum values in all physical quantities under consideration here depends sensitively on the pressure and the mirror magnetic fields. For $P = 3.5$ and 3.0×10^{-4} Torr we have in $0.0 \leq Z \leq 26.0$ cm observed extremum values of T_e, N_e, V_f, E_{rf} and B_{rf} only for $\bar{B} = 3.7, 5.5$ and 8.1×10^{-2} T. For $P = 2.0 \times 10^{-4}$ Torr we have not found extremum values in any quantity and for any of the five values of \bar{B} . For $P = 1.0 \times 10^{-4}$ Torr extrema can be observed again for the same values of \bar{B} as for $P = 3.0$ and 3.5×10^{-4} Torr, but now, the maximum of T_e is much higher (about 10 times), while the minimum of N_e is still similar as for $P = 3.0$ and 3.5×10^{-4} Torr.

Finally, we have also measured the components of the rf field (E_z, E_r, E_ϕ) as a function of Z along the axis, in the absence of plasma and at ambient pressure. They all decrease monotonically with increasing distance from the rf helix, i.e., for $0.0 \leq Z \leq 26.0$ cm and radial position $r = 0.0$ cm. The average values are $\bar{E}_z = 3.0 \times 10^{-3}$ and $\bar{E}_\phi = 11.0 \times 10^{-3}$ statvolts/cm. The value $(\bar{E}^c)^2 = (\bar{E}_z)^2 + (\bar{E}_r)^2 + (\bar{E}_\phi)^2 = 18 \times 10^{-5}$ dynes/cm² will be used to calculate the parameter p whose values determines the threshold between a linear and a nonlinear phenomenon (cf. section 4.2).

4. DISCUSSION AND PHYSICAL MODEL

4.1 - Discussion

The dips, experimentally found in the electron density and in the components of the rf electromagnetic field, are typical for the nonlinear physical phenomenon known as "caviton". Characteristic parameter of the cavitons are the relative depth $\Delta N_e/\bar{N}_e = (N_e - \bar{N}_e)/\bar{N}_e$ and the resonant width Δz . In previous work values of 20 to 50% for $\Delta N_e/\bar{N}_e$ and of 1 to 12 cm for Δz were found for the transient cavitons (4,10,16), and the minimum of N_e split up into several minima. Typical values observed in the present experiment are $\Delta N_e/\bar{N}_e = 100\%$,

$\Delta z = 2.0$ to 4.0 cm, and the minima show no further substructure. Simultaneously we observe a strong increase of the electron temperature, $\Delta T_e/T_e = (T_e - T_e^*)/T_e = 200\%$ at the spatial position $z = z^L$ of the density caviton. Other important results were confirmed: the floating potential V_f (17) is extremely sensitive to abrupt variations of the electron temperature T_e , and the temperature increases with decreasing electron density N_e (9). These results are consistent with the principal result presented in this work, i.e., stationary cavitons of large depth and small width. We have also confirmed: the electron density increases with increasing mirror magnetic field (Table II) (18), and the temperature decrease with increasing the pressure (19). This increase of density with increasing the mirror magnetic field (Table II) suggest that we may generate a density gradient when the mirror magnetic field is varying from 0.0 Tesla to the desired value of work. This is really possible since our mirror magnetic field is on only after the plasma was produced by the rf field (cf. section - 2). Therefore, this density gradient created by the mirror magnetic field, may generate the cavitons in the standard way as discussed in section-1, however in those work (cf. section 1), the rf field was applied to an unmagnetized plasma with a density gradient prepared before. It is important to observe that the local values of mirror magnetic field where the cavitons were observed are approximately equal the average values of the mirror magnetic field, cf. table I.

Finally, the values of temperature presented in this work (Table I) indicates that argon should be multiply ionized since we have enough rf power ($600W$) to do this (Maxwellian distribution of velocity) (20). However, the Langmuir probe diagnostic may detected essentially the current produced by the argon single ionized (cf. reference (20), figures 4 and 5). The average values of temperature presented are similarities with results obtained in previous work (1,2,19,21). Furthermore for a cold and tenuous plasma ($N_e \leq 10^9 \text{ cm}^{-3}$) the electron temperature may be of the order 10 to 100 eV . (22).

4.2 - Physical Model: Localized excitation of electrostatic wave and caviton formation.

It is known that an rf helix can generate slow waves if the space S between turns is much smaller than the free space wavelength λ (23). This slow wave helical structure can excite waves in the plasma if the plasma frequency ω_{pe} is higher than the rf frequency ω_{rf} , and if the electron cyclotron frequency ω_{ce} is greater than

ω_{rf} and the longitudinal component of the refraction index $N_z = c/V\phi$ is much larger than one (c is the velocity of light in the vacuum and $V\phi$ is the phase velocity of the slow wave) (24).

From our experimental setup we have $\lambda = 250 \text{ cm}$, $S = 1.25 \text{ cm}$, and $V\phi = c \sin \theta = 1.30 \times 10^9 \text{ cm/s}$, $\theta = 2.58^\circ$ is the pitch angle (12), therefore these conditions are satisfied ($(V\phi/V_{the}) = (\text{phase velocity of the slow wave/average electron thermal velocity})$ is of the order 6 to 7). Since $\lambda \gg S$, $\omega_{ce} \gg \omega_{rf}$, $N_z \gg 1$ and the plasma frequency is always higher than the rf frequency, we expect a plasma wave excitation in our system. We believe that a localized excitation of electrostatic waves may occurs in a local point of the density gradient created by the magnetic mirror where the rf frequency ω_{rf} is approximately equal to the reduced plasma frequency $\omega_{pe}^* = \omega_{pe} / \sqrt{2}$ (25). ω_{pe}^* is the local plasma frequency taken outside the caviton (Table III). Table III shows that $\omega_{pe}^* = (1-2)\omega_{rf}$, therefore resonant harmonics of ω_{rf} generates the cavitons. Furthermore, since the plasma is nonuniform the resonant harmonics of ω_{rf} which may occur in a non linear layer of the plasma can be as high as $\omega_{rf}/\omega_{pe} = 1, 2, 5/2, 3, 7/2$, and 4 , (26), therefore these values of ω_{rf}/ω_{pe} are in agreement with the values presented in this work (Table III). In this point the existence of a strong rf electromagnetic field (Figure 2) generate the stationary density cavity (Figure 1) by ponderomotive forces in the standard way (4). The cavitons traps the rf field, favoring again the excitation of electrostatic waves as well as the ponderomotive effects. This process continues until a saturation mechanism sets in.

For mean values of the mirror magnetic field higher than $\bar{B} = 1.0 \times 10^{-2} \text{ T}$ we have not observed cavitons. Reference (21) shows that for a resonance-sustained radio frequency discharge a single resonance remains for high values of $(\omega_{ce}/\omega_{rf}) = (\text{electron cyclotron frequency/rf frequency})$, while for values of ω_{ce}/ω_{rf} smaller than one a splitting of the main resonance is observed. For high values of ω_{ce}/ω_{rf} , beside the main resonance a serie of temperature peaks can be observed; however in reference (21) nothing is said about cavitons formation, or peaks of rf field, nor about the values of ω_{ce}/ω_{rf} that were used. From our experimental results we have observed peaks of temperature and also stationary cavitons, and the average values of ω_{ce}/ω_{rf} that we have used were $8 \leq \omega_{ce}/\omega_{rf} \leq 50$ but the cavitons were observed only for $8 \leq \omega_{ce}/\omega_{rf} \leq 18$.

Finally, it should be noted that the

generation of density cavities and localized electric fields in a nonuniform plasma does not require the amplitude of the electric field to be very large. The parameter that determines this nonlinear threshold is

$$p = (W_{rf} \times L / V_{the})^2 \times (\bar{E}^2) / 12(N_p T_e)$$

which can be quite large (of order 1 or larger) even for modest levels of (\bar{E}^2) . For external power levels such that $p > 1$ the formulation presented in reference (5) predicts that we have nonlinear phenomena (cavitons).

In our experimental results L = profile length scale = 26 cm and $(\bar{E}^2) = (E_z)^2 + (E_r)^2 + (E_\theta)^2 = 18 \times 10^{-5} \text{ dyne/cm}^2$ is the rf pressure. For the various value of T_e the nonlinear parameter p is the order 10 to 20 and we are well above the threshold need for nonlinear behavior.

SUMMARY

We have observed stationary cavitons of large depth and small width, in a Lisitano plasma produced and heated by a rf field in continuous wave mode and confined by a magnetic mirror, differently from previous work, where an oscillating electric field was applied to an unmagnetized plasma with a density gradient prepared beforehand (4,10). These nonlinear structures ($p > 1$) is highly stable (in time) and localized (in space) at some position which depends on the plasma conditions as pressure and mirror magnetic field (Table I). The cavitons are generated in a density gradient by electrostatic resonance in $W_{rf} = W_{pe} / \sqrt{2}$. The density gradient is created by the mirror magnetic field (Table II).

Finally, the stationarity of the caviton may be explained in terms of the equilibrium between the ponderomotive force and the thermokinetic force, however, these results as well as a mathematical model developed to explain stationary caviton taking into consideration the mirror magnetic field and the rf field will be published in somewhere else.

REFERENCE

- (1) - A.J.Balloni, S.Aihara and P.H.Sakana, paper accepted for publication in Plasma Physics and Nuclear Fusion (1988).
- (2) - G.P.Galvão and S.Aihara, Lett. Nuovo Cimento 33,140 (1982).
- (3) - D.E.Baldwin, Rev. Mod. Phys. 49,317 (1977).
- (4) - H.C.Kim, R.L.Stenzel, A.Y.Wong, Phys. Rev. Lett. 33,886(1974).
- (5) - G.J.Morales and Y.C.Lee, The Phys. of Fluids, 20,1135 (1977).
- (6) - P.DeNeef, Phys.Rev.Lett.39,997(1977)
- (7) - A.Y.Wong, P.Leung, et al, Phys.Rev. Lett. 39,1407 (1977).
- (8) - G.Lisitano: Proc. 7th Int. Conf. Ioniz.Phenm.Gases, Beograd 1,464

- (1966), and Plasma Phys. 15,457(1973).
- (9) - H.Akiyama, M.Kando, K.Minamo S. Takeda, J.Phys.S.Japan 40,839(1976).
- (10) - D.L.Eggleson, A.Y.Wong, C.B.Darrow, Phys. Fluids. 25,257(1982).
- (11) - A.J.Balloni, A.C.Jesus Paes et al, Revista Brasileira de Aplicações de Vácuo, 6,175(1986).
- (12) - S.Ramo, J.R.Whinnery and T.V.Duzer, Fields and Waves Communication. Electronics, J.Wiley, N.Y.(1965).
- (13) - F.F.Chen-"Modern Use of Langmuir Probes", Report, IPPJ(1985).
- (14) - R.H.Huddeleston, S.L.Leonard, Plasma Diagnostic Techniques, Academic Press, New York(1965).
- (15) - S.Aihara and G.Lampis, Lett.Nuovo Cimento 2, 1309(1971).
- (16) - P.Y.Cheung, A.Y.Wong et al, Phys. Rev. Lett. 48,1348 (1982).
- (17) - R.W.Mottley, Q.Machines, Chapt.2,3, Acad.Press N.Y. (1975).
- (18) - Sanborn C.Brown, Basic Data of Plasma Physics, pag. 296, The M.I.T. Press Cambridge, Massachusetts (1959).
- (19) - V.Agnelo, N.Barasi, Il.Nuovo Cimento XLIII B,2 Guigno(1966).
- (20) - A.Matsumoto, S.Aihara et al, Institut of Plasma Phys. Nagoya, Japan, Research Report, I.P.P.J. 380 Apr(1979).
- (21) - J.Tayllet, American J. Phys. 37, 423 (1969), and reference therein
- (22) - J.C.Sprott, K.A.Connor et al, Plasma Phys. 14, 269 (1972).
- (23) - R.E.Collin, Foundations for Microwave Engineering, pag. 396 - McGraw-Hill Tokyo (1966).
- (24) - V.Kopecky, J.Musil and F.Zacek, Plasma Phys. 17,1147 (1975).
- (25) - N.A.Krall and A.W.Trivelpiece, Principles of Plasma Physics, pag. 160, Int Std Edition, McGraw-Hill (1973).
- (26) - Laser Interaction and Related Plasma Phenomena, by H.Scharz and H.Hora, 4B(1976) 689.
- (27) - C.J.Morales and Y.C.Lee, Phys.Rev. Lett. 33,1534 (1974).

TABLE CAPTIONS

TABLE I

Extremum values T_e and N_e of electron temperature and their localization Z^L as well as their average value T_e and N_e in the interval $0 \leq Z \leq 26 \text{ cm}$ for various average magnetic fields \bar{B} and pressure P . B^L is the local magnetic field where the extremum values were observed.

TABLE II

Average values of electron density N_e and mean mirror magnetic field B . N_e increases with increasing \bar{B} for the various values of pressure P .

TABLE III

Values of localized reduced plasma

frequency $\tilde{\omega}_{pe}$ for which we have a localized resonance near ω_{rf} . ω_{pe} is the average plasma frequency, N_e is the local density value outside the caviton and $\omega_{rf}=7.54 \times 10^8$ is the rf. frequency.

TABLE - I

P (10 ⁻⁴ Torr)	B (10 ⁻² T)	T _e (ev)	N _e (10 cm ⁻³)	ZL (cm)	B _L (10 ⁻² T)	T _{eL} (ev)	N _{eL} (10 ⁸ cm ⁻³)
3.0	5.5	11.	9.4	7.	5.7	30.	1.8
	8.1	15.	14.	10.	10.3	42.	2.9
	3.7	11.	3.	15.	4.9	44.	0.3
3.5	5.5	10.	8.8	7.	5.7	28.	2.5
	8.1	14.	14.7	11.	10.7	34.	4.0

TABLE - II

B (10 T)	3.7	5.5	8.1	14.2	21.1
P (10 ⁻⁴ Torr)	N _e (10 cm ⁻³)				
3.0	3.0	9.4	14.0	21.0	31.0
3.5	2.2	8.0	14.6	16.0	23.6

TABLE - III

N _e (10 cm ⁻³)	ω_{pe} (10 s ⁻¹)	N _e (10 ⁸ cm ⁻³)	ω_{pe} (10 ⁸ s ⁻¹)	$\frac{\tilde{\omega}_{pe}}{\omega_{pe}}$ (10 s ⁻¹) = ω_{pe}/ω_{rf}	$\frac{\tilde{\omega}_{pe}}{N=\omega_{pe}/\omega_{rf}}$
9.4	17.3	8.	16.	11.3	1.5
14.	21.1	17.5	23.6	16.7	2.2
3.	9.8	3.	9.8	6.9	0.92
8.8	16.7	12.	19.5	13.8	1.8
14.7	21.6	18.	24.	17.	2.2

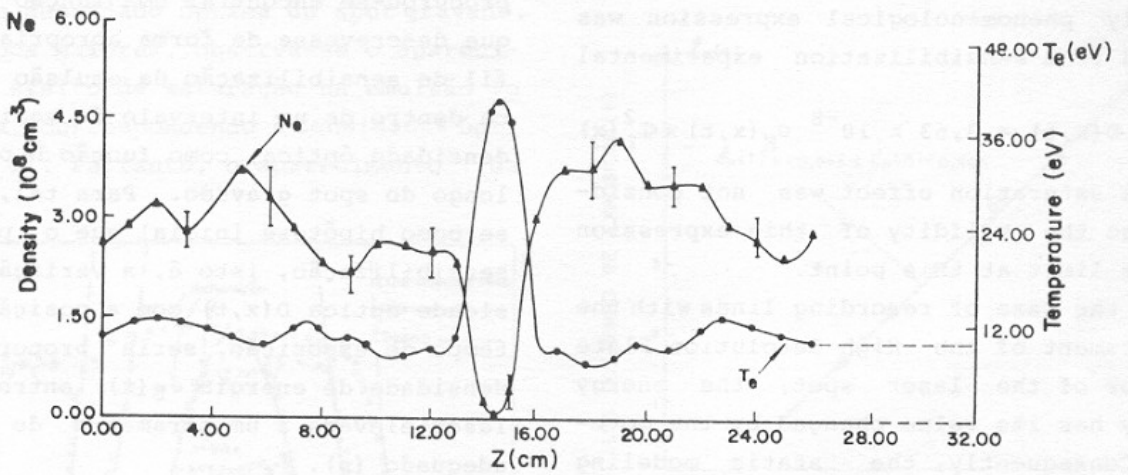


Fig. 1 - Electron density along the axis.
 $P = 3.0 \cdot 10^{-4}$ Torr $\bar{B} = 3.7 \times 10^{-2}$ T

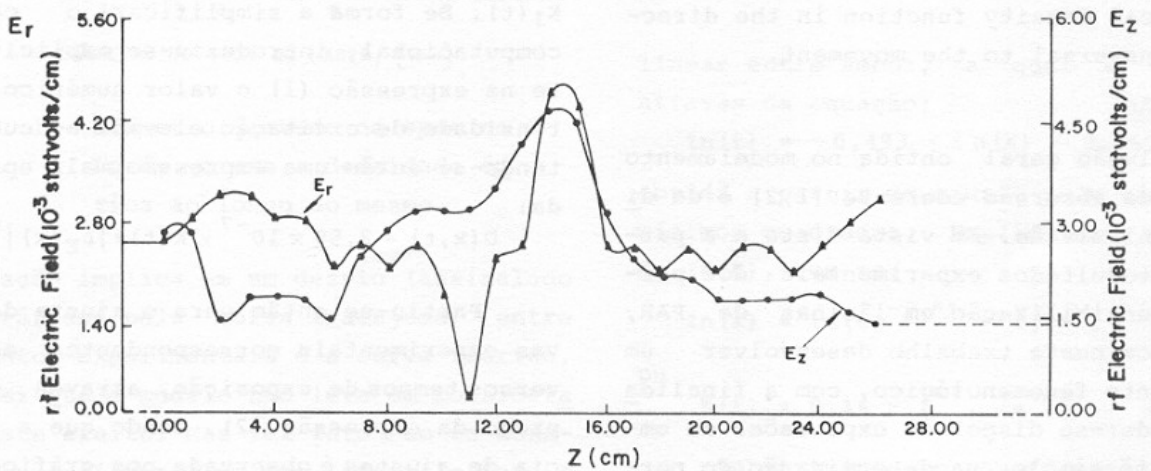


Fig. 2 - rf Electric field along the axis
 E_r = Radial electric field
 E_z = Longitudinal electric field
 $P = 3.0 \cdot 10^{-4}$ Torr $\bar{B} = 3.7 \times 10^{-2}$ T